Strength, Fracture and Complexity 11 (2018) 149–168
DOI 10.3233/SFC-180220
IOS Press

Nano-scale fracture phenomena and TeraHertz pressure waves as the fundamental reasons for geochemical evolution

Alberto Carpinteri* and Oscar Borla
Politecnico di Torino, Department of Structural, Geotechnical and Building Engineering, Corso Duca degli Abruzzi 24, 10129 Torino, Italy

Abstract. TeraHertz vibrations and pressure waves are produced at the nano-scale in solids and fluids by fracture and cavitation, respectively. They present a frequency that is close to the resonance frequency of the atomic lattices and an energy that is close to that of thermal neutrons. Original experiments performed on non-radioactive rocks under mechanical compression loading have shown repeatable neutron emissions in correspondence to micro- and macro-fracture. After these experiments, a considerable reduction in the iron content of the crushed rocks appears to be consistently counterbalanced by an increase in Al, Si, and Mg contents. At the same time, significant measurements of neutron emissions are observed at the Earth's Crust scale before and during seismic activity. In addition, several data coming from geochemistry and geomechanics have recently emphasized how tectonic activity should have been strictly connected to the most important changes in the Earth's Crust chemical composition over the last 4.5 Billion years. On these bases, the hypothesis of a new kind of low energy nuclear reactions finds confirmation and could be considered as a valid explanation for the geologic evolution of the Earth's Crust, Ocean, and Atmosphere. The same phenomenon appears to have occurred also in the chemical evolution of other planets of the Solar System like Mars, and of the Sun itself.

Keywords: TeraHertz pressure waves, nano-scale, fracture, geochemical evolution

AUTHOR COPY

1. Fracture at different scales: From Hertz to TeraHertz pressure wave frequencies

When you cut a stretched rubber band, it remains subject to rapid fluctuations for a few moments. The same phenomenon occurs in any solid body when it breaks in a brittle way, even if only partially. In the case of the formation or propagation of microcracks, such dynamic phenomenon appears under the form of longitudinal waves of expansion/contraction (tension/compression), in addition to transverse or shear waves. These are generally called pressure waves and travel at a speed which is characteristic of the medium, and, for most of the solids and fluids, presents an order of magnitude of 10^3 metre/second. On the other hand, the wavelength of pressure waves emitted by forming or propagating cracks appears to be of the same order of magnitude of crack size or crack advancement length. The wavelength can not therefore exceed the maximum size of the body in which the crack is contained and may vary from the nanometre scale (10^{-9} metres), for defects in crystal lattices such as vacancies and dislocations, up to the kilometre, in

*Corresponding author. E-mail: alberto.carpinteri@polito.it.

1567-2069/18/$35.00 © 2018 – IOS Press and the authors. All rights reserved

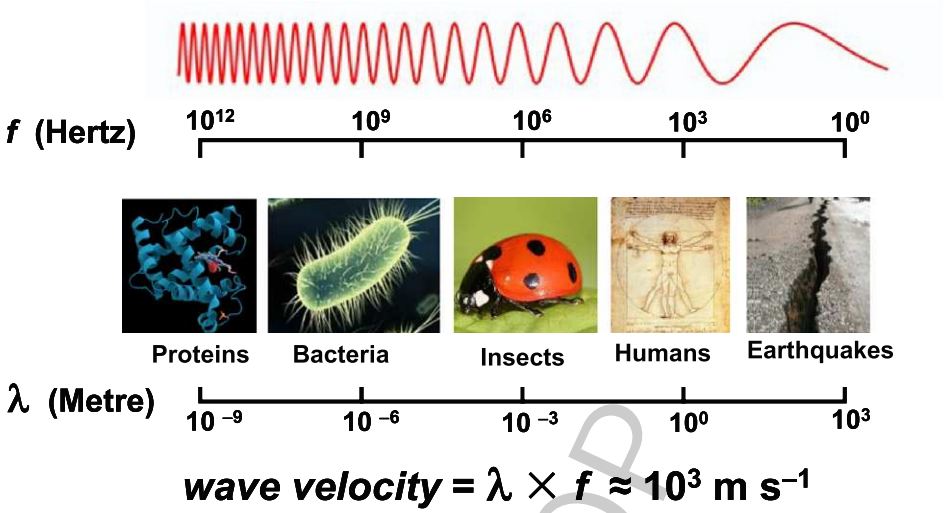

Fig. 1. Correlation between wavelength (forming crack) scale and frequency scale by assuming a constant pressure wave velocity.

the case of Earth's Crust faults. Applying the well-known relationship: frequency = speed/wavelength, one obtains the two extreme cases corresponding to the frequency of pressure waves: 10^{12} oscillations/second (TeraHertz), in the case of the formation of nanocracks, as well as one oscillation/second (Hertz), in the case of large-scale tectonic dynamics (Fig. 1) [1]. A correlation is herein considered between the wavelength scale (which coincides with the crack length scale) and the frequency scale by assuming a constant acoustic wave speed.

As fracture at the nanoscale (10^{-9} metres) emits pressure waves at the frequency scale of TeraHertz (10^{12} Hertz), so fracture at the microscale (10^{-6} metres) emits pressure waves at the frequency scale of GigaHertz (10^{9} Hertz), at the scale of millimetre emits pressure waves at the scale of MegaHertz (10^{6} Hertz), at the scale of metre emits pressure waves at the scale of kiloHertz (10^{3} Hertz), and eventually faults at the kilometre scale emit pressure waves at the scale of the simple Hertz, which is the typical and most likely frequency of seismic oscillations (Fig. 1) [1,2].

When the active cracks are still below the metre scale, pressure waves can generate Acoustic Emission (AE) in the frequency range of ultrasounds (from kilo- to MegaHertz).

With frequencies between Mega- and GigaHertz, and therefore cracks between the micron and the millimetre scale, pressure waves can generate Electromagnetic Emission (EME) of the same frequency.

When pressure waves show frequencies between Giga- and TeraHertz, and then with cracks below the micron scale, we are witnessing a phenomenon partially unexpected: pressure waves resonate with the crystal lattices and, through a complex cascade of events (acceleration of electrons, bremsstrahlung gamma radiation, photo-fission, etc.), may produce nuclear fission reactions [3–15]. It can be shown experimentally how such fission reactions emit neutrons (Neutron Emission NE), like in the well-known case of uranium-235. Note that the Debye frequency, i.e., the fundamental frequency of free vibration of crystal lattices, is around the TeraHertz, and this is not a coincidence but is simply due to the fact that the inter-atomic distance is just around the nanometre, as indeed the minimum size of the lattice defects. As the chain reactions are sustained by thermal neutrons in a nuclear power plant, so the low energy fission reactions are triggered by pressure waves that have a frequency close to the resonance frequency of the crystal lattice and an energy close to that of thermal neutrons (0.025 eV). As a matter of fact, thermal

AUTHOR COPY

Fig. 2. The two granitic orthogneiss (Luserna stone) specimens before (left) and after (right) the fracture tests.

neutrons are characterized by a frequency of 6.05 THz (according to the well-known law that links energy and frequency through the Planck's constant), which is very close to the uranium atomic lattice resonance frequency of 6.24 THz [2]. Therefore, as well as thermal neutrons can trigger fission reactions, so pressure waves with very high frequency (THz) can induce low energy fission phenomena.

Debye resonant frequencies with an order of magnitude of THz are also typical for other medium weight elements, such as Fe (7.77 THz [2]) and Ca (4.79 THz [2]), that played a fundamental role in the chemical evolution of our planet [1], as will be shown in the following.

The low energy fission reactions are often accompanied and revealed by the emission of neutrons and/or alpha particles. However, gamma rays and radioactive wastes appear to be absent in the experiments.

Ultrasonic pressure waves may in turn be produced by the most common mechanical instabilities, such as fracture in solids and turbulence in fluids. Both are hierarchical, multi-fractal, and dissipative phenomena, where cracks and vortexes, respectively, are present at the different scales. The same phenomenon appears to have occurred in several different situations and, in particular, in the chemical evolution of Earth and solar System, trough seismicity (rocky planets) and turbulent flow instability (gaseous planets and Sun) [1]. It can also explain puzzles related to the history of our planet, like the ocean formation or the primordial carbon pollution [1].

In this paper the authors, on the bases of the original experimental results obtained from non-radioactive rocks under mechanical compression loading, consider the hypothesis of low energy nuclear reactions as a valid explanation for the geological evolution of the Earth's crust, ocean, and atmosphere.

2. Neutron emission from rock specimens

After the early experiments conducted at the National Research Council of Italy (CNR) [16], soliciting with ultrasounds aqueous solutions of iron salts, the research group of the Politecnico di Torino has conducted fracture experiments on solid samples, using iron-rich rocks like granite, basalt, and magnetite, as well as marble, mortar enriched with iron dioxide, and steel [1,17–24].

In the preliminary experiment, two specimens of Luserna stone were tested (Fig. 2). Both were of the same size and shape, measuring $6 \times 6 \times 10\ \text{cm}^3$. The neutron measurements obtained exceed the background level by approximately one order of magnitude, when catastrophic failure occurred (Fig. 3).

In more recent experiments, cylindrical specimens with different size and slenderness were selected, instead of prismatic specimens as in the preliminary tests. Different types of detectors have demonstrated the presence of significant neutron emissions, in some cases by different orders of magnitude higher than

AUTHOR COPY

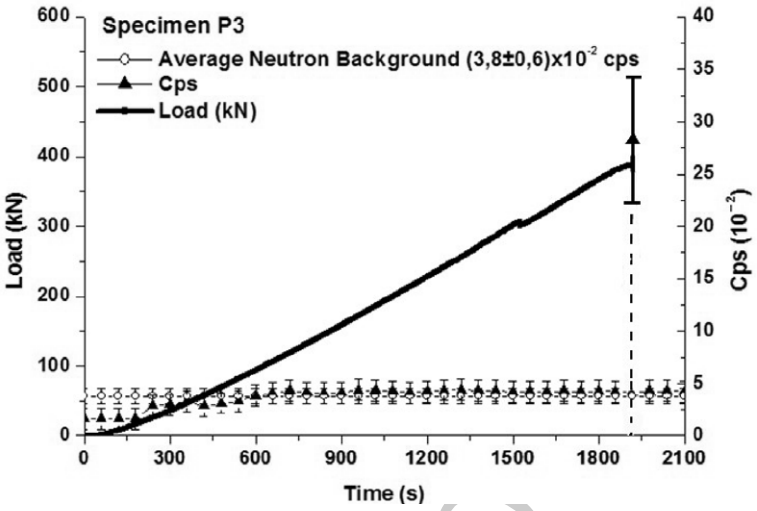

Fig. 3. Load vs. time and cps curve for test specimen of granitic orthogneiss.

Table 1
Neutron emission level during fracture and cavitation of different materials

Material	Neutron emissios
LIQUIDS (cavitation)	
Iron chloride solution	Up to 2.5 times the background level
SOLIDS (fracture)	
Steel	Up to 2.5 times the background level
Granite	Up to 10^1 times the background level
Basalt	Up to 10^2 times the background level
Magnetite	Up to 10^3 times the background level
Marble	Background level

AUTHOR CC

the usual environmental background. The neutron flux was found to depend, besides on the iron content, on the size of the specimen through the well-known brittleness size effect: larger sizes imply a higher brittleness, i.e. a more relevant strain energy release, and therefore more neutrons.

The results obtained from iron chloride liquid solutions subjected to cavitation and from non-radioactive rocks subjected to fracture, fatigue, and ultrasounds are summarized in Table 1 [1,16–24]. Liquids during cavitation were characterized by neutron emissions up to 2.5 times the background level [16]. The same neutron emission level was obtained in the case of steel specimens subjected to compression or tension up to the final failure. For granitic rocks, presenting a small amount of iron content (Fe 1.5%), a neutron emission up to one order of magnitude greater than the background level was detected during several tests [1,17–24]. For basalt and magnetite, where the iron concentration is much higher (Fe 15% and 72.5%, respectively), neutron emissions respectively up to 10^2 times and 10^3 times the background level were measured during fracture experiments [1]. As regards marble, no neutron emissions greater than the background level were observed during fracture experiments [1].

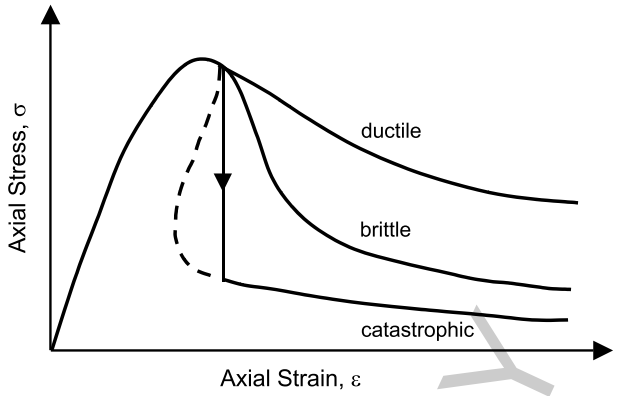

Fig. 4. Ductile, brittle, and catastrophic behaviour.

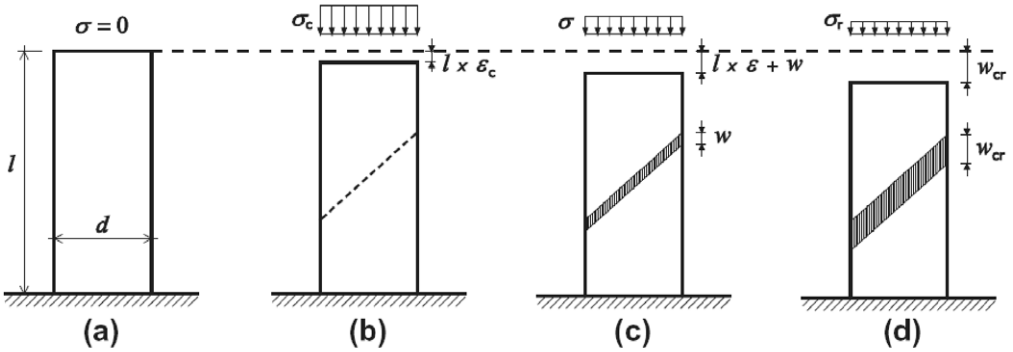

Fig. 5. Subsequent stages in the deformation history of a specimen in compression.

3. Ductile, brittle, and catastrophic behaviour of rocks in compression

Experimental data from rocks tested in compression generally indicate that this is a brittle material, since it exhibits a rapid decrease in load carrying capacity when deformed beyond the peak load. When the softening diagram is very steep, or even shows simultaneously decreasing strain and stress values, the material is said to present a snap-back or catastrophic behaviour. This is in contrast with ductile materials which retain considerable strength beyond the peak as shown in Fig. 4 [25–27].

Damage localisation strongly affects the behaviour of heterogeneous materials in compression, with particular regard to the post-peak regime [28]. As a result, it is well-established that the classical stress vs. strain constitutive laws, which assume a homogeneous response along the specimen axis, are strongly affected by the size and the slenderness of the specimen.

A significant step toward the definition of a scale independent constitutive law for quasi-brittle materials has been done by Carpinteri et al. [29], with the proposal of the Overlapping Crack Model (OCM). The main assumption of the OCM is that the localisation process, whatever may be its origin, is modelled by means of a fictitious interpenetration of the two parts of the specimen, that exhibit an elastic behaviour.

Let us consider the specimen subjected to uniaxial compression test shown in Fig. 5. The application of the OCM permits the mechanical response to be represented by three subsequent phases.

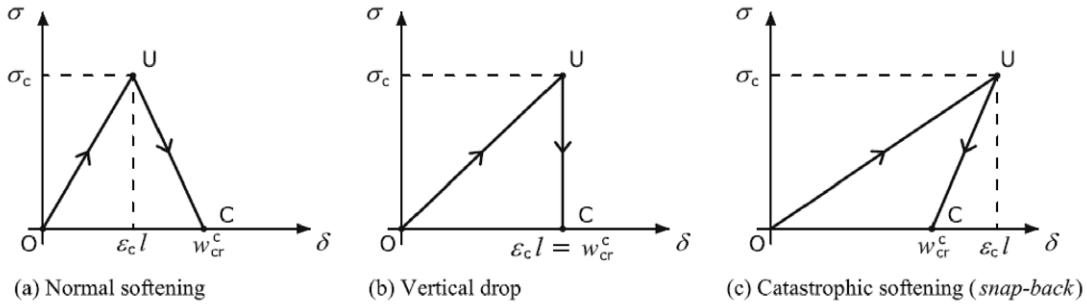

Fig. 6. Stress–displacement response of a specimen in compression.

A first stage where the behaviour is mainly characterised by the elastic modulus of the material: a simple linear elastic stress–strain law can be assumed (see Fig. 5b). The displacement of the upper side of the specimen is:

$$\delta = \varepsilon l = \frac{\sigma}{E} l, \quad \text{for } \varepsilon \leq \varepsilon_c.$$

By approaching the compressive strength, the microcracks interact forming macrocracks, and, eventually, localising on a preferential surface.

A second stage where, after reaching the ultimate compressive strength, σ_c, the inelastic deformations are localised in a crushing band. The behaviour of this zone is described by a softening law, whereas the bulk material still behaves elastically (see Fig. 5c). The total shortening of the specimen can be computed as the sum of the elastic deformation and the interpenetration displacement w. While the crushing zone overlaps, the elastic zone expands at progressively decreasing stresses.

When $\delta \quad w_{\rm cr}$, in the third stage, the material in the crushing zone is completely damaged and is able to transfer only a constant residual stress, σ_r (see Fig. 5d). As a result, the transition from softening to snap-back instability in the load vs. displacement global response, experimentally obtained by increasing the specimen slenderness and/or by varying the mechanical properties, can be correctly predicted. In particular, the softening process is stable under displacement control only when the slope $\mathrm{d}\delta/\mathrm{d}\sigma$ in the post-peak regime is negative (Fig. 6a). On the contrary, the snap-back instability is obtained when the slope $\mathrm{d}\delta/\mathrm{d}\sigma$ of the softening branch becomes positive, Fig. 6c.

From the point of view of energy, the OCM has also been proved to be very effective in determining the amount of released energy during the complete loading process [30]. In particular, more information on the modalities of energy release and the development of cracking patterns can be obtained from the monitoring of the fracto-emissions (AE, EME, and NE). The application of suitable devices on or close to the surface of specimen permits to detect the energy emissions induced by the crack formation and propagation.

The typical shape of the load vs. displacement curve, when the global unstable behavior is fully captured, e.g. by controlling the compression test by means of the circumferential expansion instead of the longitudinal deformation, is that shown in Fig. 7a. However, this very brittle mechanical response can be observed also under tension and bending loading conditions, when brittle materials are tested in large and/or slender specimens. The behavior shown in Fig. 7a is consequent to the fact that the energy dissipated through material damage is less than all the elastic energy stored in the body. In this case, the portion of energy that is not dissipated by material damage (area E in Fig. 7a) is abruptly emitted leading

AUTHOR COPY

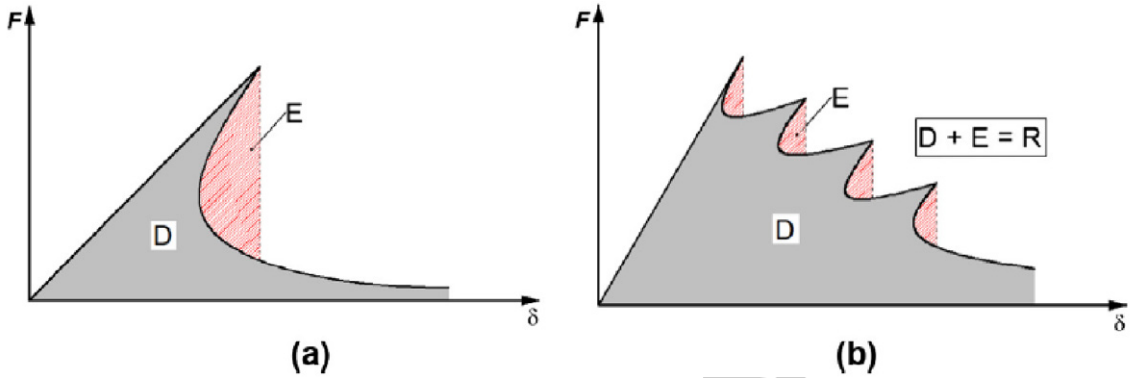

Fig. 7. Load–displacement curves representing: (a) a catastrophic failure (single snap-back); (b) a global softening behavior perturbed by multiple local instabilities (snap-back).

to dynamic vibrations, with propagation of mechanical pressure waves that, depending on their frequency, can trigger the emission of AE, EME, or NE [1].

Of course, this portion of energy will be dissipated also through material viscosity, kinetic energy of fragments, heat, etc.

From the diagram in Fig. 7a, therefore, three different energy components can be distinguished: the energy dissipated (D) by material damage (gray area), the emitted elastic energy (E) (pink area), and the total released energy (R), which is the sum of the two previous areas (D + E = R).

Certainly, global snap-back instabilities take place only under specific conditions (large sizes and slendernesses, and/or brittle materials), whereas in most of the cases a more stable response, represented by a softening behavior, is obtained.

However, even in such cases, local discontinuities, which are an indication of snap-back or snap-through instabilities, are usually noticed in heterogeneous materials such as aggregative and fiber-reinforced materials. Such local phenomena, that are evident at a microscale level, are due to the fact that cracks grow in a discontinuous manner, with sudden propagations and arrests due to the bridging action of the secondary phases as well as by the rise and coalescence of microcracks in the process zone [31,32]. A load–displacement curve representative of a global softening behavior perturbed by multiple local instabilities is shown in Fig. 7b. Each drop in the load carrying capacity occurring in the post-peak phase is related to a sudden crack propagation due, for instance, to the rupture of a reinforcing fiber. Then, the load carrying capacity is partially recovered following a path with a reduced stiffness. From the energetic point of view, each local instability is due to the emission of a surplus of elastic energy, which is not dissipated by the material damage (pink areas in Fig. 7b). This emitted energy can be detected by the AE, EME, and NE sensors.

4. Chemical evolution of our planet and its reproduction in the fracture mechanics laboratory

The low energy fission reactions have also been able to give an answer to some puzzles related to the history of our planet. It has been shown how these phenomena that would have occurred between 3.8 and 2.5 Billion years ago, during the period of formation and most intense activity of tectonic plates, have resulted in the splitting of atoms of certain elements, which were so transformed into other lighter

AUTHOR COPY

Table 2
Biotite: Fe, Al, Si, Mg, and K weight percentage mean values on external and fracture surfaces

	External surface mean value (wt%)	Fracture surface mean value (wt%)	Increase/decrease with respect to biotite	Increase/decrease with respect to the same element
Fe	21.2	18.2	3%	14%
Al	8.1	9.6	+1.5%	+18%
Si	18.4	19.6	+1.2%	+6%
Mg	1.5	2.2	+0.7%	+46%
K	6.9	7.1	No variations	No variations

ones. Since the product-elements, i.e., the fragments of the fissions, appear to be stable isotopes, all the excess neutrons are therefore emitted. Several of the most abundant chemical elements have been involved in similar transformations, like a part of magnesium that transformed into carbon, forming the dense atmospheres of the primordial terrestrial eras. In a similar way, calcium depletion contributed to the formation of oceans as a result of fracture phenomena in limestone rocks.

These transformations, that have lasted for Billion years in the Earth's Crust, have been reproduced in the laboratory in a fraction of a second by crushing different rock samples [1,17–24, 33]. We were able to confirm, through advanced micro-chemical analyses, the most relevant compositional variations described above at the geological and planetary scales: the transformation of iron into aluminum, or into magnesium and silicon (in iron-rich natural rocks), as well as the transformation of calcium and magnesium into other lighter elements including carbon (in the samples of marble). Such variations are shown to be not modest at all.

In particular, Energy Dispersive X-ray Spectroscopy (EDS) analysis was performed on different sample spots of external or fracture surfaces belonging to the granite specimens used in the fracture experiments, in order to get averaged information about possible changes in their chemical composition. The measurement precision is in the order of magnitude of 0.1%. The results for phengite and biotite (minerals with an higher Fe concentration in granite) show that the relative reduction in the iron abundance (25%) seems to be counterbalanced by the increment in lighter elements such as Al, Si, and Mg [20–23]. Similar investigations were also performed on different samples of basalt and magnetite [1]. For the former, a significant decrement in the iron content (4%) is counterbalanced by the increment in lighter elements such as Si and Mg [1]. On the other hand, the results for magnetite are even more evident. The decrease in Fe concentration is nearly equal to 30%, while the appearance of Al and Mn, previously absent, represents a very impressive result, as well as the increment in Si and O [1].

In Fig. 8a–d the results for Fe, Al, Si, and Mg concentrations of biotite crystalline phase are shown. In this case, the iron decrease is about 3.0%, from 21.2% (external surface) to 18.2% (fracture surface) (Fig. 8a). At the same time, Al content variations show an average increase of about 1.5% (Fig. 8b). In Fig. 8c and 8d it is shown that, in the case of biotite, also Si and Mg contents present considerable variations. The mass percentage of Si changes from a mean value of 18.4% (external surface) to a mean value of 19.6% (fracture surface), with an increase of 1.2% (Fig. 8c). Similarly, the mean value of Mg concentration changes from 1.5% (external surface) to 2.2% (fracture surface), with an increase of 0.7% (Fig. 8d). Therefore, the iron decrease (3.0%) in biotite is counterbalanced by an increase in aluminum (+1.5%), silicon (+1.2%), and magnesium (+0.7%) [20–23] (Table 2).

AUTHOR COPY

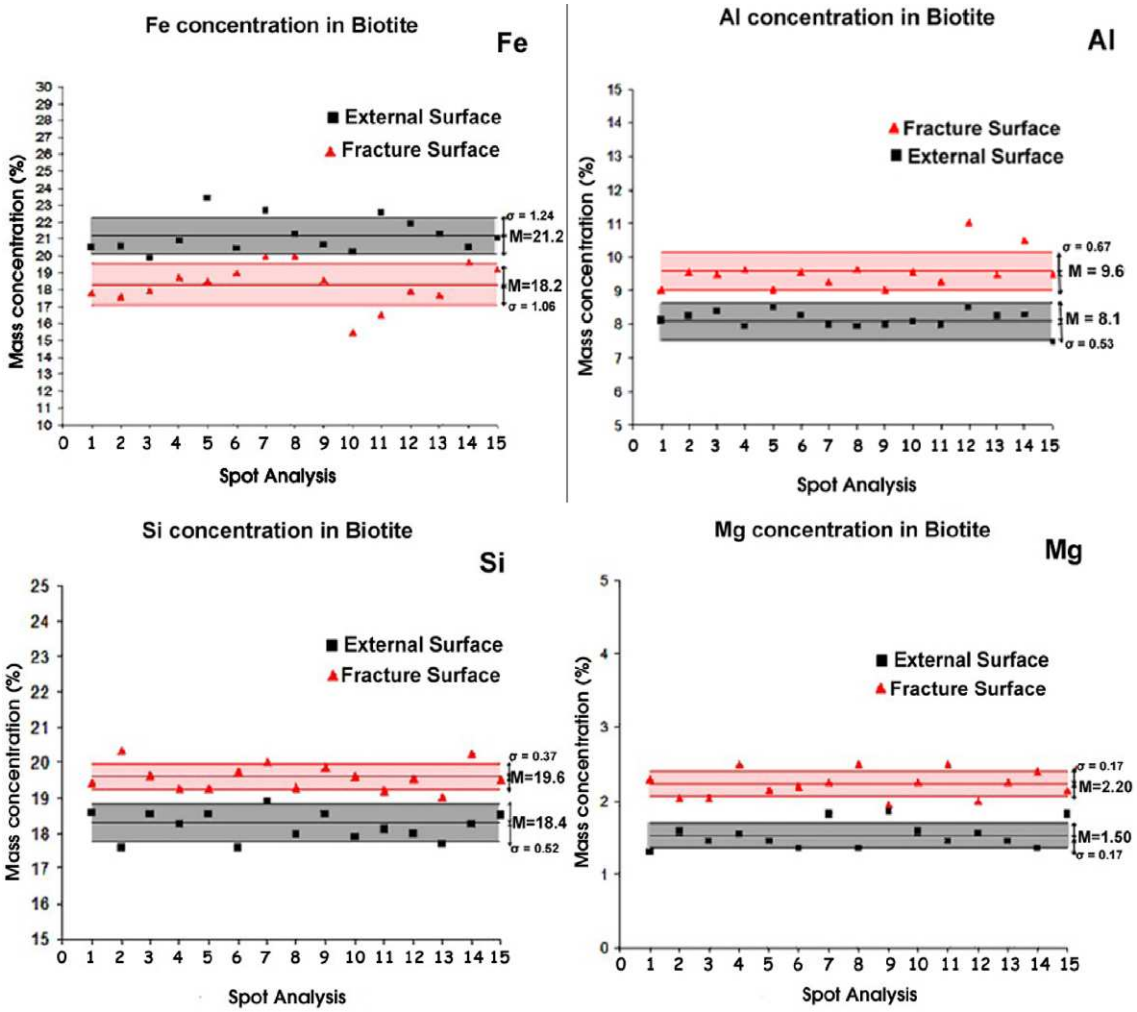

Fig. 8. EDS results of Fe (a), Al (b), Si (c) and Mg (d) concentrations in biotite analysed on samples coming from fractured specimens of granite.

Similar results were obtained for Carrara Marble specimens [1]. In this case, X-ray Photoelectron Spectroscopy (XPS) quantitative compositional analyses were carried out in order to detect any variation in chemical composition after the brittle failure of cylinder specimens [1]. XPS survey scan (pass energy of 187.85 eV) of Carrara Marble surfaces was performed. Thirty measurements on external surface, and twenty on fracture surface were performed and analysed. In Table 3, the results for the O, Ca, Mg, and C concentrations are shown. It can be observed that the distributions of O, Ca, and Mg concentrations on the external surface show average values respectively equal to 45.8%, 13.4%, and 0.7%. In the same diagrams, the distributions of O, Ca, and Mg concentrations on the fracture samples show significant variations. The mean value of the measurements performed on fracture surfaces is respectively equal to 36.8%, 9.8%, and 0.3%, and they are considerably lower than the mean values on the external surface. The Carbon mass percentage increase of 13.0% is approximately equal to the total decrease in O, Ca, and

Table 3
Carrara Marble: Ca, Mg, O, and C weight percentage mean values on external and fracture surfaces

	External surface mean value (wt%)	Fracture surface mean value (wt%)	Increase/decrease with respect to marble	Increase/decrease with respect to the same element
Ca	13.4	9.8	3.6%	26%
Mg	0.7	0.3	0.4%	57%
O	45.8	36.8	9.0%	19%
C	40.1	53.1	+13.0%	+32%

Mg. The average value of C concentrations changes from 40.1% on the external surface to 53.1% on the fracture surface.

4.1. Iron depletion versus carbon pollution

Over the last century, most recent scientific disciplines such as cosmology, astrophysics, and geology, have tried to answer questions concerning the origin of the Earth and the Universe [34]. Such questions have now given place to interrogatives concerning the substance that composes the Universe, the heterogeneous distribution of the main elements on the Earth, and their evolution in time [34–38].

Significant evidences, such as relatively abrupt changes in element abundances [35–37], the Great Oxidation Event (G.O.E.) between 2.7 and 2.4 Gyr ago [1], the strong iron and nickel depletions in Earth's crust and oceans [39], the transition from a mafic to a sialic condition in the Continental Crust [33,37,40], the present level of CO_2 and N_2 concentrations in the Earth's atmosphere [1], and the appreciable precursory role of CO_2 and neutron emissions before relevant earthquakes [41–48], are just some of the major events pertaining to the dynamics and the evolution of chemical element abundances in Earth's crust, oceans, and atmosphere, that still remain unsolved. Recent investigations and new instruments for data analysis led to study these unexplained phenomena more deeply.

Another question that still remains unanswered concerns the non-homogeneous composition of Oceanic and Continental Crusts. The 85% of the Earth's volcanic eruptions take place at the sea bottom in correspondence to mid ocean-ridges [49]. These submarine volcanoes generate the solid underpinnings of all the Earth's oceans (Oceanic Crust) [35–37,50]. Comparing the data presented in the literature concerning the composition of the two different types of terrestrial crust, it can be noted that the iron concentration changes from 8%, in the Oceanic Crust, to 4% in the Continental one. Analogously, nickel changes from 0.03% in the Oceanic Crust to 0.01% in the Continental one (about a threefold decrease). Vice versa, Si, Al, and Na vary from 24%, 7%, and 1% in the Oceanic Crust, to 28%, 8%, and 2.9% in the Continental Crust, respectively [35–37]. Considering that approximately 50% of the Continental Crust has originated, over the last 3.8 Gyr, from the Oceanic Crust subduction [35,36,49,50], the considerable variations in the composition of the Oceanic with respect to the Continental Crust would seem to remain a mystery [49].

In this context, the location of Al and Fe mineral reservoirs seems to be inexplicably connected to the geological periods when different continental zones were formed [35,51,52]. This fact would seem to suggest that our planet has undergone a continuous evolution from the most ancient geological regions, which currently reflect the continental cores that are rich in Fe reservoirs, to more recent or contemporary areas of the Earth's Crust where the concentrations of Si and Al oxides present very high

AUTHOR COPY

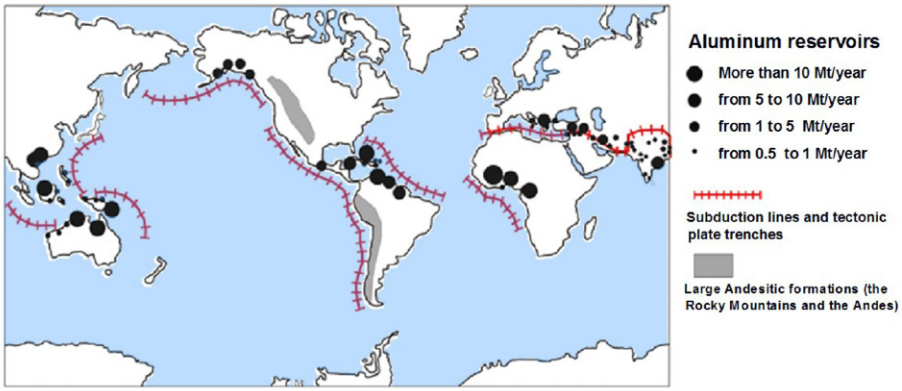

Fig. 9. The largest aluminum (bauxite) reservois.

mass percentages [35,51,52]. At the same time, the concentrations of Al-oxides and andesitic formations (the Rocky Mountains and the Andes), are shown together with the most important subduction lines, tectonic plate trenches and rifts (see Fig. 9) [35,51]. The bauxite mine locations show that the largest concentrations of Al reservoirs can be found in correspondence to the most seismic areas (Fig. 9). The main iron mines are instead exclusively located in the oldest and interior parts of continents (formed through the eruptive activity of the proto-Earth), in geographic areas with a reduced seismic risk and always far from the main fault lines.

Many other questions concern the fact that the Earth, in contrast to the other rocky planets of our Solar System, has shown a strong compositional evolution over the last 4.57 Billion years. From 4.0 to 2.0 Gyr ago, in fact, Fe could be considered as one of the most common bio-essential elements required for the metabolic action of all living organisms [37–39]. Today, the deficiency of this nutrient suggests it as a limiting factor for the development of marine phytoplankton and life on Earth [37,39]. Elements such as Fe and Ni in the Earth's protocrust had higher concentrations during the Hadean (4.5–3.8 Gyr ago) and Archean (3.8–2.5 Gyr ago) periods compared to the present values [35–40]. The Si and Al concentrations instead were lower than they are today [35–38,40]. The estimated concentrations of Fe, Ni, Al, and Si in the Hadean and Archean Earth's protocrust and in the present Earth's Continental Crust are reported in Fig. 10. The data for the Hadean period (4.5–3.8 Gyr ago) are referred to the composition of Earth's protocrust, considering the assumptions made by Foing [53] and by Taylor and Mc Lennan [36]. The most abrupt changes in element concentrations shown in Fig. 10 appear to be intimately connected to the tectonic activity of the Earth. The vertical drops in the concentrations of Fe and Ni, as well as the vertical jumps in the concentrations of Si and Al, occurred 3.8 Gyr ago, coincide with the time that many scientists have pointed out as the beginning of tectonic activity on our planet. The subsequent step-wise transitions occurred 2.5 Gyr ago coincide with the period of the Earth's most intense tectonic activity [35,36].

From the data reported in Fig. 10, a decrease of 7% in Fe and 0.2% in Ni concentrations can be observed between the Hadean period (4.5–3.8 Gyr ago) and the Archean period (3.8–2.5 Gyr ago) [35–38,40,54]. At the same time, Al and Si concentrations increase of 3% and 2.4% respectively. Similarly, a global decrease of 4.8% in the concentrations of Fe (4%) and Ni (0.8%) and a global increase of about 3.4% in the concentrations of Si (2.4%) and Al (1%) are shown between the Archean period (3.8–2.5 Billion years ago) and more recent times. The balances between heavier (Fe and Ni) and lighter (Si and Al) elements could be considered as perfectly satisfied, if we take into account a stepwise increase in Mg

AUTHOR COPY

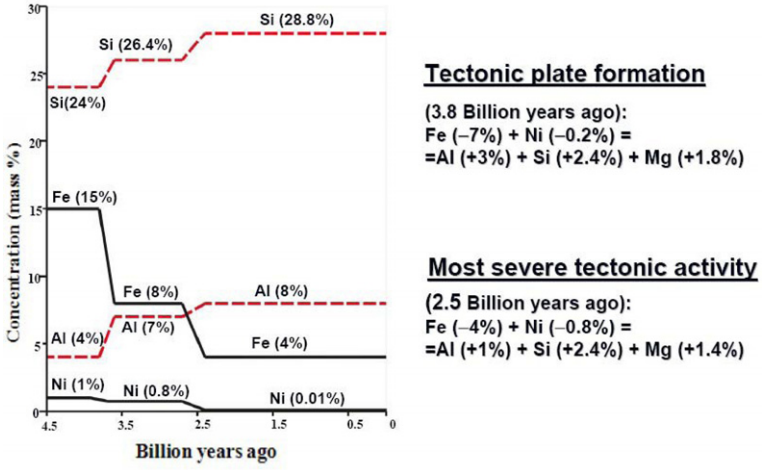

Fig. 10. The estimated concentrations of Fe, Ni, Al, and Si in the Hadean and Archean Earth's protocrust and in the Earth's Continental Crust.

similar to that of Si over the Earth's lifetime. This Mg increase cannot be deduced from the geological data of ancient sediments but will be explained in the following considering not only the geochemical changes that involve the Earth's Crust but also other important traces that can be recognized in the evolution of the Earth's atmosphere.

On the bases of the experimental results and evidences reported in Figs 8, 9, 10, the low energy fission reactions 1 and 2 reported in Table 4 should have occurred during fracture phenomena.

Considering the present natural abundances of the major elements such as Fe, Al, Si, Mg, Na, Ni in the Continental Crust [35–38,40,54], it is possible to conjecture that the additional nuclear reactions 3–6 reported in Table 4 could have taken place in correspondence to plate collision and subduction.

The large concentrations of granite minerals, such as quartz and feldspar in the Earth's Continental Crust, and to a lesser extent of magnesite, halite, and zeolite (MgO, Na_2O, Cl_2O_3), and the low concentrations of magnetite, hematite, bunsenite and cobaltite minerals (composed predominantly of Fe, Co, and Ni molecules), could be ascribed to the low energy fission reactions 1–6. The same transition, between the basaltic composition of the Oceanic Crust to the sialic composition of the Continental Crust may be explained by reactions 1–6.

In particular, reactions 1, 2, 5 seem to be the cause of the abrupt variations shown in Fig. 10. The overall 12% decrease in the heavier elements (Fe and Ni) is perfectly balanced by the Al, Si and Mg increase (12%) over the last 3.8 Billion years. At 3.8 Billion years ago, in fact, we can consider the following balance: Fe (7%) + Ni (0.2%) = Al (+3%) + Si (+2.4%) + Mg (+1.8%). Analogously, at 2.5 Billion years ago we have: Fe (4%) + Ni (0.8%) = Al (+1%) + Si (+2.4%) + Mg (+1.4%). The increments in Si and Mg are not exactly the same due to the fact that Si is involved at the same time in reactions 2 and 5, and for the different atomic mass numbers of the two elements. However, as mentioned before, the Mg increase, due to the low energy fission reaction 2, cannot be revealed from geological data. The explanation is that Mg can be considered also as a starting element of further low energy fission reactions as shown in the case of reaction 7. This reaction provides important explanations concerning the composition of atmosphere in the past geological eras and the present natural carbon emissions [33]. The virtual increase of 3.2% in Mg, involved, at the same time, in reactions 2 and 7, could explain the

Table 4
Low energy fission reactions obtained by direct evidence of EDS and XPS analyses of fractured specimens and emerging from the evolution of the continental Earth's Crust

	Earth's crust evolution
1	$Fe_{26}^{56} \rightarrow 2Al_{13}^{27} + 2$ neutrons
2	$Fe_{26}^{56} \rightarrow Mg_{12}^{24} + Si_{14}^{28} + 4$ neutrons
3	$Fe_{26}^{56} \rightarrow Ca_{20}^{40} + C_{6}^{12} + 4$ neutrons
4	$Co_{27}^{59} \rightarrow Al_{13}^{27} + Si_{14}^{28} + 4$ neutrons
5	$Ni_{28}^{58} \rightarrow 2Si_{14}^{28} + 2$ neutrons
6	$Ni_{28}^{58} \rightarrow Na_{11}^{23} + Cl_{17}^{35}$
	Atmosphere evolution, ocean formation and origin of life
7	$Mg_{12}^{24} \rightarrow 2C_{6}^{12}$
8	$Mg_{12}^{24} \rightarrow Na_{11}^{23} + H_{1}^{1}$
9	$Mg_{12}^{24} \rightarrow O_{8}^{16} + 2H_{1}^{1} + He_{2}^{4} + 2$ neutrons
10	$Ca_{20}^{40} \rightarrow 3C_{6}^{12} + He_{2}^{4}$
11	$Ca_{20}^{40} \rightarrow K_{19}^{39} + H_{1}^{1}$
12	$Ca_{20}^{40} \rightarrow 2O_{8}^{16} + 4H_{1}^{1} + 4$ neutrons

high level of carbon in the primordial atmosphere and, consequently, the higher pressure with respect to the present one. Taking into account a density of 3.6×10^3 kg m ^{3} and a mean thickness of 60 km for the Hadean and Archean Crusts, the mass of the protocrust involved in reaction 7 is equal to 3.4×10^{21} kg and implies a pressure on the Earth's surface of about 660 atm (considering the Earth's surface equal to 5.1×10^{14} m^2 like today). This pressure is very high if compared with that of the present Earth's atmosphere but can be considered a plausible value for the composition of the Earth's primordial atmosphere between 3.8 and 2.5 Billion years ago. Several authors, in fact, describe a primordial Earth's atmosphere saturated in carbon, with a pressure of several hundred atmospheres. In particular Liu [55] suggests a value of 650 atm for the proto-atmosphere, composed principally by carbon gasses and H_2O and similar to that of Mars and Venus [54,56]. After the intense tectonic activity that involved our planet during Adean and Archean periods, the high carbon concentration, principally due to reaction 7, started to decrease. This fact can be explained considering the planetary air leak of elements, such as H, He, and carbon, that has affected the atmosphere during the Earth's lifetime [56].

Low energy fission reaction 7 can also be put into correlation to the increase in seismic activity that has occurred over the last century [57]. Very recent evidence has shown CO_2 emissions in correspondence to seismic activity: significant changes in the emission of carbon dioxide were recorded in a geochemical station at El Hierro, in the Canary Islands, before the occurrence of seismic events during the year 2004. Appreciable precursory CO_2 emissions were observed to start before seismic events of relevant magnitude and to reach their maximum values some days before the earthquakes [48]. From this point of view, the evidence emerging from the XPS analyses, performed at the laboratory scale on marble, that the percentage of oxygen, calcium and magnesium totally decreases (13.0%) and that of C increases

AUTHOR COPY

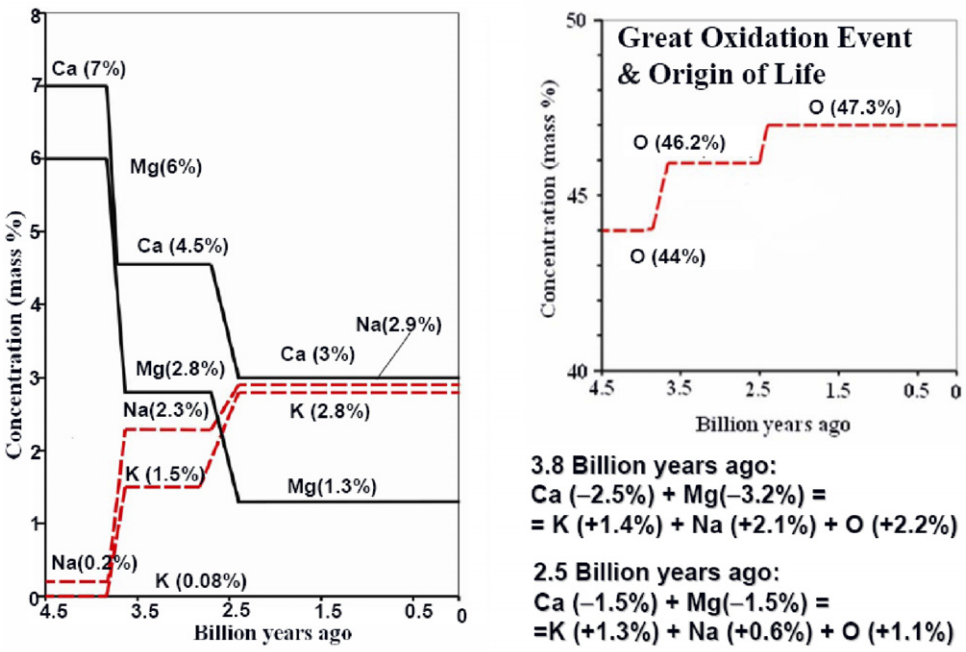

Fig. 11. The variations in mass percentage for Mg, Ca, Na, K, and O in the Hadean and Archean Earth's protocrust and in the Earth's Continental Crust.

(+13.0%), emphasizes how reactions 7, and 10 may take place in calcareous rocks. In fact, no neutron emission does not imply absence of nuclear transmutations.

4.2. Calcium depletion versus ocean formation

In addition to Fe, Ni, Si, Al, and Mg, it is possible to consider also the other most abundant elements such as Ca, Na, K, and O, which are involved in the Earth's Crust chemical evolution. The variations in mass percentage for Mg, Ca, Na, K, and O in the Hadean and Archean Earth's protocrust and in the Earth's Continental Crust are reported in Fig. 11, analogously to Fig. 10 [35,36,40]. The decrease in the mass concentrations of Mg and Ca is balanced by an increase in Na, K, and O, during the Earth's lifetime. In particular, between the Hadean and the Archean eras, and between the latter and more recent times, it is possible to observe an overall decrease of 4.7% for Mg and 4.0% for Ca. This decrease in the two alkaline earth metals (Mg and Ca) seems to be nearly perfectly balanced by the increase in the concentrations of the two alkaline metals, Na and K (which have increased by 2.7% each), and by a total increase of 3.3% in O, which has varied from 44% to 47.3% (the latter being the present Oxygen concentration in the Earth's Crust (Fig. 11)). Also in this case, the greatest chemical changes in the Earth's Crust are strictly connected to the most intense tectonic activity in the planet.

Plate tectonics and the connected subduction phenomena seem to involve the Earth's Crust compositional evolution and the changes in the most abundant chemical elements. These phenomena have often been ignored by orthodox views. At the same time, the macroscopical evidence emerging from Figs 9, 10, and 11 cannot be explained only by the chemical element migrations or by the differentiation process that should have taken place during the Earth's formation [35,36].

AUTHOR

According to the traditional explanation, this differentiation caused the heavy metals (iron, nickel, and other ferrous elements) to be concentrated in the core of the planet, whereas the light elements (oxygen, silicon, aluminum, calcium, potassium, sodium, etc.) were enriched in the upper layers of the Earth: the Mantle and, in particular, the Crust [35,36]. Not everything, however, occurs simply according to density. In the authors' vision, the traditional approach cannot explain how the oceanic crust, characterized by a more basaltic composition, could generate the margins of the continents, which are composed by the lighter sialic elements. In other words, if the mechanism were only that traditionally proposed, the oceanic crust would be principally sialic as the continental one. Moreover, the traditional approach cannot explain other contradictory evidences such as that regarding the Uranium and Thorium concentrations. These two very heavy elements should be expected to be abundant in the core, but, on the contrary, they are concentrated in the crust and the mantle of our planet.

At the same time, the temporal correlation between most important tectonic activities on Earth and most evident chemical changes in the crust, together with the nearly perfect chemical concentration balances, suggest that alternative interpretations of the Earth's Crust evolution should be taken into account. Plate tectonics and high-frequency pressure waves seem to imply the chemical evolution. This last interpretation is even more convincing if we consider recent measurements, performed by Kuzhevskij et al. [41,42], Antonova et al. [43], Volodichev et al. [44], Sigaeva et al. [45], and Carpinteri et al. [46,47], in correspondence to seismic activity. The results presented in these papers lead to consider also the Earth's Crust, in addition to cosmic rays, as being a relevant source of neutron flux variations. Neutron emissions exceeded the neutron background up to 1000 times in correspondence to earthquakes with a Richter magnitude equal to the 4th degree [44]. These measurements could be considered connected to the previous changes in the Earth's Crust and to mechanical phenomena of fracture, crushing, fragmentation, comminution, erosion, friction, occurring during seismic events.

Reaction 7, reported in Table 4, is not the only one that involves Mg as a starting element. From a close examination of the data reported in Fig. 11, it is possible to conjecture a series of low energy fission reactions, involving Mg, Ca, Na, K, O, C and H, that could represent the real origin of the sharp fluctuations of these chemical elements in the evolution of the Earth's Crust (see reactions 7–12 in Table 4). Considering reactions 8, 9, 11, and 12, an overall decrease in alkaline earth metals (Mg and Ca) of about 8.7% is balanced by a nearby equal increase in Na, K, and O (see Fig. 11). At 3.8 Billion years ago, we have the following balance (see Fig. 11 and Table 4): Ca (2.5%) + Mg (3.2%) = K (+1.4%) + Na (+2.1%) + O (+2.2%). At 2.5 Billion years ago, on the other hand, we have: Ca (1.5%) + Mg (1.5%) = K (+1.3%) + Na (+0.6%) + O (+1.1%). Also in this case, the mass percentage variations in the major elements of the Earth's Crust could be perfectly explained considering this new kind of nuclear fission reactions (see Fig. 11).

In particular, the global decrease in Ca (4.0%) can be counterbalanced by an increase in K (2.7%), reaction 11, and in H_2O (1.3%), reaction 12. Considering the mass of the proto-crust equal to 1.08×10^{23} kg, the decrease of about 1.3% in Ca concentration corresponds to 1.40×10^{21} kg. This value is very close to the mass of water in the oceans 1.35×10^{21} kg (considering a global ocean surface of 3.60×10^{14} m^2 and an average depth of 3950 m). In this way, reaction 12 could be considered as responsible for the formation of oceans during the Earth's life time. These last considerations seem to be even more important taking into account the recent results from Europe's Rosetta mission about the origin of water on the planet Earth. The evidences coming from the exploration of the Comet 67P returned significant difference comparing the water in comets with the water we have on our planet leading to exclude the extraterrestrial origin of the ocean [58].

AUTHOR COPY

5. Compositional evolution of Mars and the Sun triggered by fracture and turbulence

The surprising findings that have emerged from analysis under the electron microprobe have highlighted how low energy fission reactions can be used to explain the geological evolution, the composition of the proto-atmosphere, the decrease in Ni and Fe in the oceans, and many other phenomena during the life of our planet.

Similar hypotheses can be formulated for the planet Mars, as the violent tectonic and volcanic activity it experienced in the Noachian Period, and the sporadic tectonic events that still today take place, have resulted in a surface marked by faults and signs of earthquakes [59,60]. In this connection, mention should be made to the fact that Mars is commonly known as the "red planet" because of the characteristic red colour of its surface. This colour results from the iron oxide, FeO, that covers much of the planet's crust and is the second most common compound in it [36]. This large quantity of Fe – around 15% by mass, as compared with 7.8% in the Earth's oceanic crust [36], which is richer in iron than the continental crust (4.0%) – raises interesting questions about the planet's evolution and the role that unexpected nuclear reactions may have had in this process.

Evidence of the possible role of these reactions can be provided by the high correlation between the areas showing extensive signs of tectonic activity and the concentration of Fe on the surface.

The exploratory Mars Odyssey mission also analyzed the neutron emission data by the HEND He_3 High Energy Neutron Detector carried on the spacecraft to measure epithermal neutrons in an energy range of 0.4 eV–100 keV[61–63]. In both cases, the correlations between neutron emissions, Fe concentrations and fault locations on the planetary crust are surprisingly close.

Here, the underlying assumption which explains the high correlation between these data is that Fe is not the starting element of a low energy fission reaction – as it is on Earth – but is the resultant of reactions that involve elements with a higher atomic number as the starting elements (Ni, Sn, Cu). In the scientific literature, moreover, several studies report an increase in the concentration of Fe on the Red Planet's surface over the last 4.57 Billion years [36,60,64,65]. At the same time, a number of authors report a sizeable decrease in elements such as Cu, Ni, Co, Mo, In, Zn, and Sn [36,64].

In particular, the absolute increase in Fe can be evaluated from the approximately 14% concentration in the Noachian crust to today's 15%, a relative increase of around 1% corresponding to about 2.15 $\times 10^{20}$ kg of Mars' crust. Likewise, the data for Ni concentrations indicate a roughly equivalent decrease in this element, passing from a concentration of around 1% in the Noachian Period to a negligible or near-zero concentration in Mars' present-day crust. This is thus an absolute decrease of about 100% and a relative decrease of 1% [36].

As has been assumed for other elements in the case of Earth's Crust, this evidence suggests that the following reaction took place:

$$\mathrm{Ni}_{28}^{58} \rightarrow \mathrm{Fe}_{26}^{56} + 2\mathrm{H}_{1}^{1}.$$

This reaction could explain the anomalous increase in the Fe concentration and the corresponding decrease in Ni by the same amount in terms of mass.

5.1. Kelvin–Helmholtz instability and its role in the compositional evolution of the Sun

Kelvin–Helmholtz instability is a type of turbulent flow instability that arises when different layers of fluid are in motion relative to each other. It was discovered and investigated by Lord Kelvin [66] and by Helmholtz [67], and later by Rayleigh. The simplest example that can be imagined in two dimensions is

AUTHOR COPY

that of a perfect fluid present in two adjacent regions of space: in the first region, the fluid is at rest, while in the second it moves at constant velocity. If a small disturbance is introduced at the boundary separating the two regions, fluid particles that were at rest (i.e., with zero velocity) will be moved to the region at finite velocity (and vice versa). This creates an instability: the amplitude of the disturbance continues to increase, and the particles in the two regions will mix together, forming vortices and causing the original configuration to be lost [66,67]. In this simple case, a configuration such as that which has just been described is always unstable, however small the initial disturbance may be [66,67]. Less rare than might be thought, this phenomenon is often found in nature and can be readily seen with the naked eye. An example are the distinctive wave- like formations that clouds sometimes show if subjected to particular air currents travelling at different speeds.

Kelvin–Helmholtz instability phenomena are thus very frequent on our planet, and studies of their effects have led over the years to the development of models that can predict transitions from laminar to turbulent flow [66,67].

Moreover, it has recently been observed that Kelvin–Helmholtz instability phenomena habitually take place also on the Sun's surface and in the so-called "solar corona". As was indicated earlier, these phenomena may be associated in some way with cavitation and hence with low energy fission reactions.

The Sun is a medium-small star consisting essentially of hydrogen and helium [68], as well as traces of heavier elements such as C, O, Li and Be [68]. Recent studies of the composition of the Sun's surface have indicated that, contrary to what might be expected from considering these elements as the result of nuclear fusion and from the standard models of a star's evolution, elements such as Li [69] and Be [70] are much less abundant than predicted. In evaluating the differences between the present composition of the Sun and that of the proto-Sun, it can be seen that the concentrations of Li are 160 times lower than they were 4.57 Billion years ago [69], which is not what the canonical models predict [69]. Likewise, the concentrations of Be are also lower than predicted. The depletion of these elements is normally associated with convective phenomena that transport them from the surface to hotter areas near the core, where they are destroyed by high temperatures and pressures. However, these convective phenomena are not sufficient to explain such low concentrations of Li and Be on the Sun's surface [69]. It can thus be assumed that the low Li and Be content of the Sun's surface is associated with anomalous fission reactions that, through Kelvin-Helmholtz instability, transform Li and Be into lighter elements as follows:

$$\mathrm{Be}_4^9 \rightarrow 2\mathrm{He}_2^4 + 1 \text{ neutron}$$

$$\mathrm{Be}_4^9 \rightarrow \mathrm{Li}_3^6 + \mathrm{H}_1^1 + 2 \text{ neutrons}$$

$$\mathrm{Li}_3^6 \rightarrow \mathrm{He}_2^4 + \mathrm{H}_1^1 + 1 \text{ neutron.}$$

6. Conclusions

A series of fracture experiments on natural rocks has recently demonstrated that the TeraHertz pressure waves, produced in solids and fluids by mechanical instabilities, are able to induce fission reactions on medium weight elements with neutron and/or alpha particle emissions. The same phenomenon appears to have occurred in several different situations and to explain puzzles related to the history of our planet, like the ocean formation or the primordial carbon pollution.

Considering the entire life of our planet and all the most abundant chemical elements, it can be seen how ferrous elements have dramatically decreased in the Earth's Crust (12%), as well as at the same time aluminium, silicon, and carbon have increased (+12%). Similarly, alkaline-earth elements have

AUTHOR COPY

strongly decreased (8.7%), whereas alkaline elements (+5.4%) and oxygen (+3.3%) have increased. The appearance of a 3.3% oxygen represents the well-known Great Oxidation Event, a phenomenon that led to the formation of oceans on our planet.

Moreover, the temporal correlation between most important tectonic activities on earth and most evident chemical changes in the crust, together with the nearly perfect chemical concentration balances, suggest that an alternative interpretation of the Earth's Crust evolution should be taken into account. Plate tectonics and high-frequency pressure waves seem to imply the geochemical evolution. Similar evidence may be observed in Mars crust and atmosphere and in Sun surface due to tectonic-volcanic activity in the former case and turbulent flow instability (Kelvin–Helmholtz instability) in the latter.

Conflict of interest

None to report.

AUTHOR COPY

References

[1] A. Carpinteri, G. Lacidogna and A. Manuello (eds), *Acoustic, Electromagnetic, Neutron Emissions from Fracture and Earthquakes*, Springer International Publishing, AG Switzerland, 2015.
[2] N.W. Ashcroft and D.N. Mermin, *Solid State Physics*, Cengage Learning, Delhi, 2013.
[3] P.W. Bridgman, The breakdown of atoms at high pressures, *Physical Review* **29** (1927), 188–191.
[4] R.E. Batzel and G.T. Seaborg, Fission of medium weight elements, *Physical Review* **82** (1951), 607–615.
[5] C.B. Fulmer et al., Evidence for photofission of iron, *Phys. Rev. Lett.* **19** (1967), 522–523.
[6] A. Widom, J. Swain and Y.N. Srivastava, Neutron production from the fracture of piezoelectric rocks, *J Phys. G: Nucl. Part. Phys.* **40** (2013), 15006: 1–8.
[7] A. Widom, J. Swain and Y.N. Srivastava, Photo-disintegration of the iron nucleus in fractured magnetite rocks with magnetostriction, *Meccanica* **50** (2015), 1205–1216.
[8] P.L. Hagelstein, D. Letts and D. Cravens, Terahertz difference frequency response of PdD in two-laser experiments, *J Cond. Mat. Nucl. Sci.* **3** (2010), 59.
[9] P.L. Hagelstein and I.U. Chaudhary, Anomalies in fracture experiments and energy exchange between vibrations and nuclei, *Meccanica* **50** (2015), 1189–1203.
[10] N.D. Cook, *Models of the Atomic Nucleus*, 2nd edn, Springer, Dordrecht, 2010.
[11] K. Diebner, Fusionsprozesse mit hilfe konvergenter stosswellen – einige aeltere und neuere versuche und ueberlegungen, *Kerntechnik* **3** (1962), 89–93.
[12] B.V. Derjaguin et al., Titanium fracture yields neutrons?, *Nature* **34** (1989), 492.
[13] M.F. Fujii et al., Neutron emission from fracture of piezoelectric materials in deuterium atmosphere, *Jpn J Appl Phys, Pt.1* **41** (2002), 2115–2119.
[14] A. Carpinteri, A. Manuello, D. Veneziano and N.D. Cook, Piezonuclear fission reactions simulated by the lattice model, *Journal of Condensed Matter Nuclear Science* **15** (2015), 149–161.
[15] U. Lucia and A. Carpinteri, GeV plasmons and spalling neutrons from crushing of iron-rich natural rocks, *Chemical Physics Letters* **640** (2015), 112–114.
[16] F. Cardone and R. Mignani, Possible observation of transformation of chemical elements in cavitated water, *Int. J. Mod. Phys.* **B 17** (2003), 307–317.
[17] A. Carpinteri, F. Cardone and G. Lacidogna, Piezonuclear neutrons from brittle fracture: Early results of mechanical compression tests, *Strain* **45** (2009), 332–339.
[18] F. Cardone, A. Carpinteri and G. Lacidogna, Piezonuclear neutrons from fracturing of inert solids, *Physics Letters A* **373** (2009), 4158–4163.
[19] A. Carpinteri, O. Borla, G. Lacidogna and A. Manuello, Neutron emissions in brittle rocks during compression tests: Monotonic vs. cyclic loading, *Physical Mesomechanics* **13** (2010), 268–274.

[20] A. Carpinteri, G. Lacidogna, A. Manuello and O. Borla, Energy emissions from brittle fracture: Neutron measurements and geological evidences of piezonuclear reactions, *Strength, Fracture and Complexity* **7** (2011), 13–31.
[21] A. Carpinteri, A. Chiodoni, A. Manuello and R. Sandrone, Compositional and microchemical evidence of piezonuclear fission reactions in rock specimens subjected to compression tests, *Strain* **47**(Suppl. 2) (2011), 282–292.
[22] A. Carpinteri, G. Lacidogna, A. Manuello and O. Borla, Piezonuclear fission reactions in rocks: Evidences from microchemical analysis, neutron emission, and geological transformation, *Rock Mechanics and Rock Engineering* **45** (2012), 445–459.
[23] A. Carpinteri, G. Lacidogna, O. Borla, A. Manuello and G. Niccolini, Electromagnetic and neutron emissions from brittle rocks failure: Experimental evidence and geological implications, *Sadhana* **37** (2012), 59–78.
[24] A. Carpinteri, G. Lacidogna, A. Manuello and O. Borla, Piezonuclear fission reactions from earthquakes and brittle rocks failure: Evidence of neutron emission and non-radioactive product elements, *Experimental Mechanics* **53** (2013), 345–365.
[25] A. Carpinteri, Cusp catastrophe interpretation of fracture instability, *Journal of the Mechanics and Physics of Solids* **37** (1989), 567–582.
[26] A. Carpinteri, A catastrophe theory approach to fracture mechanics, *International Journal of Fracture* **44** (1990), 57–69.
[27] A. Carpinteri and N. Pugno, Are scaling laws on strength of solids related to mechanics or to geometry?, *Nature Materials* **4** (2005), 421–423.
[28] M.D. Kotsovos, Effect of testing technique on the post-ultimate behaviour of concrete in compression, *Mater. Struct.* **16** (1983), 3–12.
[29] A. Carpinteri, M. Corrado, G. Mancini and M. Paggi, The overlapping Crack Model for uniaxial and eccentric concrete compression tests, *Mag. Concr. Res.* **61** (2009), 745–757.
[30] A. Carpinteri, G. Lacidogna, M. Corrado and E. Di Battista, Cracking and crackling in concrete-like materials: A dynamic energy balance, *Engineering Fracture Mechanics* **155** (2016), 130–144.
[31] A. Carpinteri and I. Monetto, Snap-back analysis of fracture evolution in multi-cracked solids using boundary element method, *Int. J. Fract.* **98** (1999), 225–241.
[32] A. Carpinteri and R. Massabò, Continuous vs discontinuous bridged-crack model for fiber-reinforced materials in flexure, *Int. J. Solids Struct.* **34** (1997), 2321–2338.
[33] A. Carpinteri and A. Manuello, Geomechanical and Geochemical Evidence of Piezonuclear Fission Reactions in the Earth's Crust, *Strain* **47** (2010) 8 18.267–281.
[34] E. Kolb, *Blind watchers of the sky: The people and ideas that shaped our view of the universe*, Oxford University Press, Oxford, 2000.
[35] G. Favero and P. Jobstraibizer, The distribution of aluminum in the Earth: from cosmogenesis to Sial evolution, *Coordination Chemistry Reviews* **149** (1996), 367–400.
[36] S.R. Taylor and S.M. McLennan, *Planetary Crusts: Their composition, origin and evolution*, Cambridge University Press, Cambridge, 2009.
[37] A.D. Anbar, Elements and evolution, *Science* **322** (2008), 1481–1482.
[38] C. Doglioni, Interno della Terra, Treccani, Enciclopedia Scienza e Tecnica (2007), 595–605.
[39] K.O. Buesseler et al., Ocean iron fertilization moving forward in a sea of uncertainty, *Science* **319** (2008), 162.
[40] A.A. Yaroshevsky, Abundances of chemical elements in the Earth's crust, *Geochem. Int.* **44**(1) (2006), 54–62.
[41] B.M. Kuzhevskij, O.Yu. Nechaev, E.A. Sigaeva and V.A. Zakharov, Neutron flux variations near the Earth's Crust. A possible tectonic activity detection, *Nat. Hazards Earth Syst. Sci.* **3** (2003), 637–645.
[42] B.M. Kuzhevskij, O.Y. Nechaev and E.A. Sigaeva, Distribution of neutrons near the Earth's surface, *Nat. Hazards Earth Syst. Sci.* **3** (2003), 255–262.
[43] V.P. Antonova, N.N. Volodichev, S.V. Kryukov, A.P. Chubenko and A.L. Shchepetov, Results of detecting thermal neutrons at Tien Shan High Altitude Station, *Geomagn. Aeron.* **49** (2009), 761–767.
[44] N.N. Volodichev, B.M. Kuzhevskij, O.Y. Nechaev, M.I. Panasyuk, A.N. Podorolsky and P.I. Shavrin, Sun–Moon–Earth connections: The neutron intensity splashes and seismic activity, *Astron. Vestn.* **34**(2) (2000), 188–190.
[45] E. Sigaeva et al., Thermal neutrons'observations before the Sumatra earthquake, *Geophys. Res. Abstr.* **8** (2006), 00435.
[46] A. Carpinteri and O. Borla, Fracto-emissions as seismic precursors, *Engineering Fracture Mechanics* **177** (2017), 239–250.
[47] A. Carpinteri and O. Borla, Acoustic, electromagnetic, and neutron emissions as seismic precursors: The lunar periodicity of low-magnitude seismic swarms, *Engineering Fracture Mechanics* (2018). doi:10.1016/j.engfracmech.2018.04.021.
[48] E. Padron et al., Changes in the diffuse CO2 emission and relation to seismic activity in and around El Hierro, Canary Islands, *Pure Appl. Geophys.* **165** (2008), 95–114.
[49] P.B. Kelemen, The origin of the land under the sea, *Sci. Am.* **300**(2) (2009), 42–47.
[50] R.M. Hazen et al., Mineral evolution, *Am. Mineral* **93** (2008), 1693–1720.

AUTHOR COPY

[51] World Mineral Resources Map. Available at http://www.mapsofworld.com/world-mineralmap.htm. Last accessed Oct 2009.
[52] Key Iron Deposits of the World. Available at http://www.portergeo.com.au/tours/iron2002/-iron2002depm2b.asp. Last accessed Oct 2009.
[53] B. Foing, Earth's childhood attic, *Astrobiol. Mag.* (2005) http://link.springer.com/article/10.1007%2FBF01732017#.
[54] F. Egami, Minor elements and evolution, *J. Mol. Evol.* **4**(2) (1975), 113–120.
[55] L. Liu, The inception of the oceans and CO2-athmosphere in the early history of the Earth, *Earth Planet Sci. Lett.* **227** (2004), 179–184.
[56] C.D. Catling and K.J. Zahnle, The planetary air leak, *Sci. Am.* **300**(5) (2009), 24–31.
[57] K. Aki, Strong motion seismology, *Earthquakes: Observation, Theory and Interpretation*, in: H. Kanamori and E. Boschi (eds), North Holland Pub. Co, Amsterdam, 1983, pp. 223–250.
[58] K. Altwegg et al., 67P/Churyumov-Gerasimenko, a Jupiter family comet with a high D/H ratio, *Science* (2014). doi:10.1126/science.1261952.
[59] W.J. Morgan, Convection plumes in the lower mantle, *Nature* **230** (1971), March 5, 1971.
[60] W.K. Hartmann and G. Neukum, Cratering chronology and the evolution of Mars, *Space Science Reviews* **96** (2001), 165–194.
[61] I. Mitrofanov et al., Maps of subsurface hydrogen from the high energy neutron detector, Mars Odyssey, *Science* **297** (2002), 78–81.
[62] M. Knapmeyer et al., Working models for spatial distribution and level of Mars' seismicity, *J. Geophys. Res.* **111** (2006), E11006. doi:10.1029/2006JE002708.
[63] W.V. Boynton, Concentration of H, Si, Cl, K, Fe and Th in the low - and mid - latitude regions of Mars, *J. Geophys. Res.* **112** (2007), E12S99. doi:10.1029/2007JE002887.
[64] H. Wanke, Chemistry, accretion, and evolution of Mars, *Space Sci. Rev.* **56** (1991), 1–8.
[65] G. Faure and T.M. Mensing, *Introduction to planetary science: The geological perspective*, Springer, Dordrecht, 2007.
[66] Lord Kelvin (William Thomson), Hydrokinetic solutions and observations, *Philosophical Magazine* **42** (1871), 362–377.
[67] Hermann von Helmholtz, Über discontinuierliche Flüssigkeits-Bewegungen [On the discontinuous movements of fluids], *Monatsberichte der Königlichen Preussische Akademie der Wissenschaften zu Berlin [Monthly Reports of the Royal Prussian Academy of Philosophy in Berlin]* **23** (1868), 215–228.
[68] S. Basu and H.M. Antia, Helioseismology and solar abundances, *Phys. Rep.* **457** (2008), 217–283.
[69] P. Baumann et al., Lithium depletion in solar-like stars: No planet connection, *Astron. Astrophys.* (2010). doi:10.1051/0004-6361/201015137.
[70] X. Da-run and D. Li-cai, Beryllium depletion in the solar atmosphere, *Chin. Astron. Astrophys.* **27** (2003), 1–3.

AUTHOR COPY